Covalent triazine framework/carbon nanotube hybrids enabling selective reduction of CO_2 to CO at low overpotential

Electronic Supplementary Information

Andreas Laemont[a], Sara Abednatanzi[a], Parviz Gohari Derakshandeh[a], Florian Verbruggen[b], Erika Fiset[b,], Qing Qin[c], Kevin Van Daele[d], Maria Meledina[e,f], Johannes Schmidt[g], Martin Oschatz[c,h], Pascal Van Der Voort[a], Korneel Rabaey[b], Markus Antonietti[c], Tom Breugelmans[d] and Karen Leus[a,*]

[a.] COMOC - Center for Ordered Materials, Organometallics and Catalysis, Department of Chemistry, Ghent University, 9000 Ghent, Belgium.

[b.] CMET- Center for Microbial Ecology and Technology, Department of Biotechnology, Ghent University, 9000 Ghent

[c.] Max Planck Institute of Colloids and Interfaces, Colloid Chemistry, Research Campus Golm, Am Mühlenberg 1, 14476 Potsdam, Germany

[d.] ELCAT – Applied Electrochemistry & Catalysis, Faculty of Applied Engineering, University of Antwerp, 2610 Antwerp, Belgium

[e.] Separation and Conversion Technology, Flemish Institute for Technological Research (VITO), Boeretang 200, Mol 2400, Belgium

[f.] RWTH Aachen University, Central Facility for Electron Microscopy, D-52074 Aachen, Germany

[g.] Forschungszentrum Jülich GmbH, Ernst Ruska-Centre (ER-C 2), D-52425 Jülich, Germany

[h.] Institut für Chemie − Funktionsmaterialien, Technische Universität Berlin, Hardenbergstraße 40, 10623 Berlin, Germany

[i.] Institute of Chemistry, University of Potsdam, Karl-Liebknecht-Str. 24-25, D-14476 Potsdam, Germany

[j.] Electronic Supplementary Information (ESI) available: [^{1}H NMR, FTIR, Raman, XRD, XPS, ADF-STEM-EDX, ICP-MS, LSV, CA,]. See DOI: 10.1039/x0xx00000x

* corresponding author, karen.leus@ugent.be

Table of contents

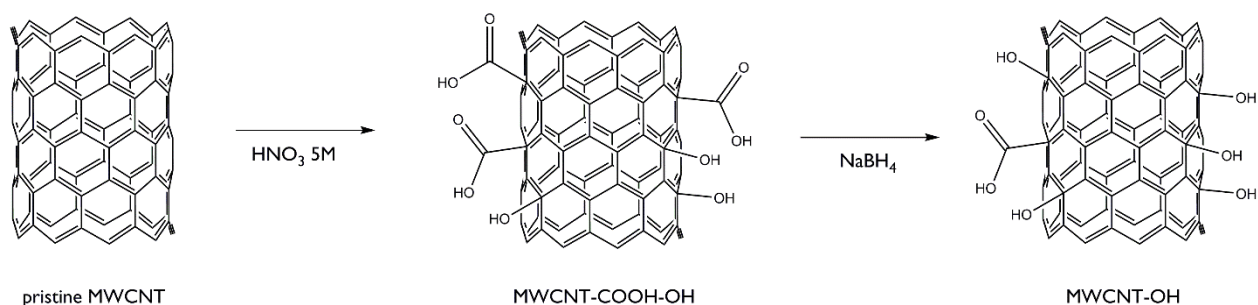# I. Synthesis and characterization of the catalyst

Synthesis of MWCNT-OH

Figure S1: Acidic oxidation of pristine MWCNTs, followed by reduction using NaBH$_4$, yielding hydroxylfunctionalized carbon nanotubes (MWCNT-OH)
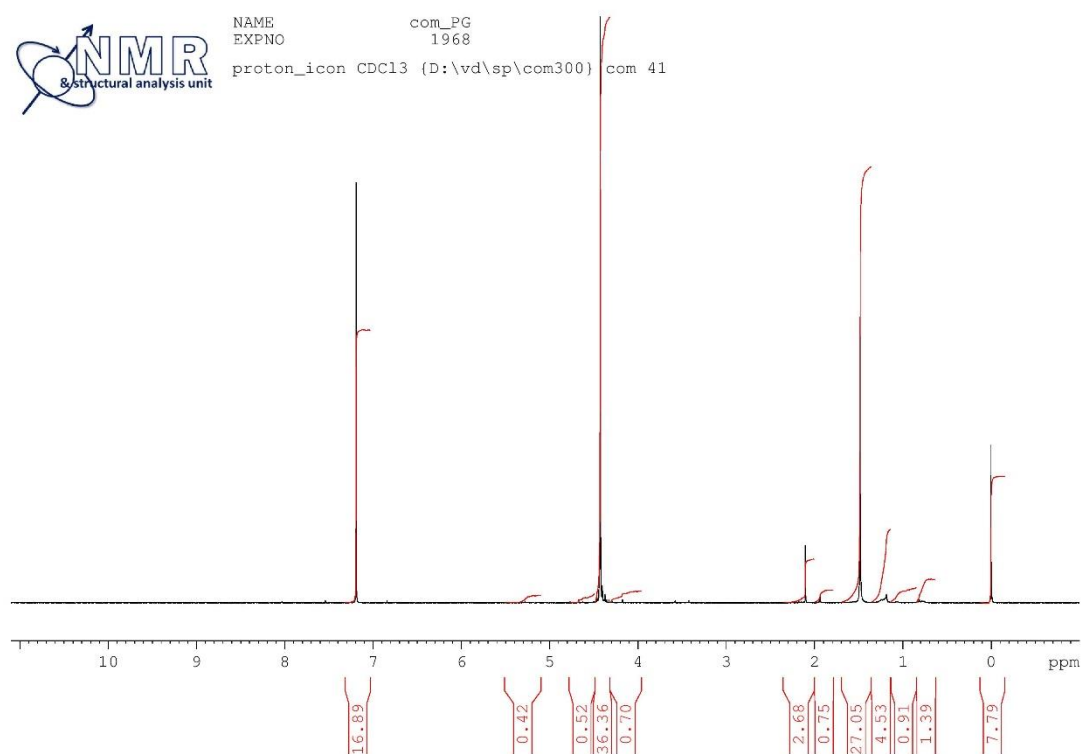
NMR

Figure S2: ^{1}H NMR spectrum of hexa-azatriphenylentrimethoxytrinitrile

Synthesis of the CTFs

2,6-pyridine-dicarbonitrile

ZnCl$_2$
500°C

pyCTF

terephtalonitrile

ZnCl$_2$
400°C

CTF1

hexa-azatriphenylenetrimethoxytrinitrile
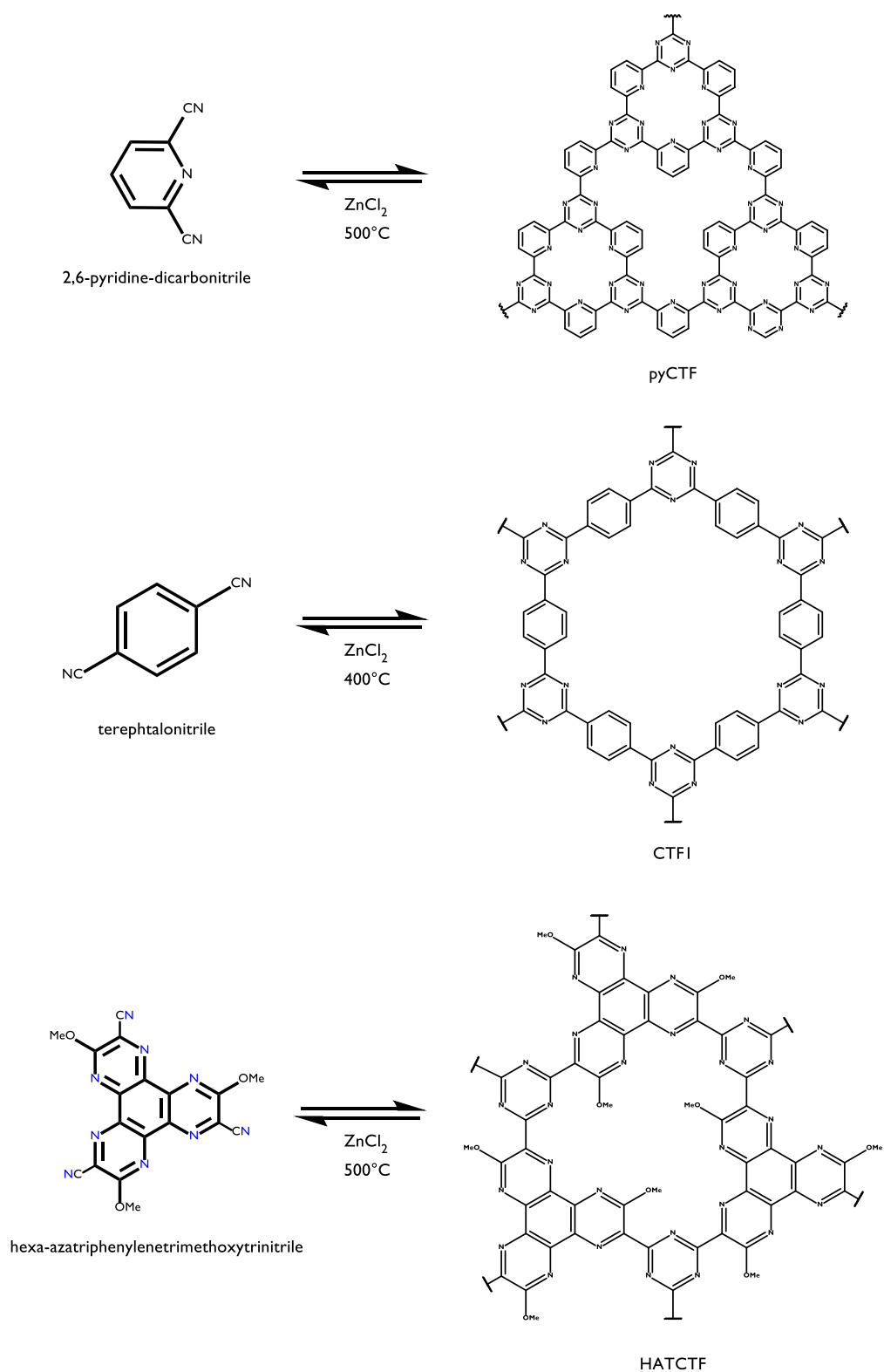
ZnCl$_2$
500°C

HATCTF

Figure S3: Ionothermal synthesis of the different CTFs

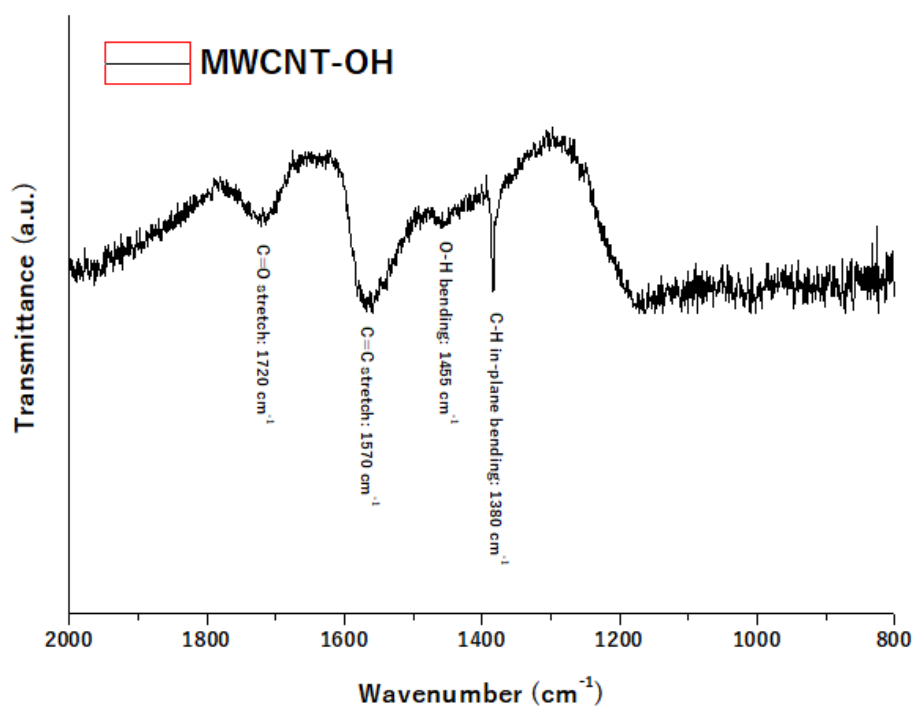# Attenuated Total Reflectance (ATR) Infrared Spectroscopy

Figure S4: FTIR-ATR spectrum detail of MWCNT-OH

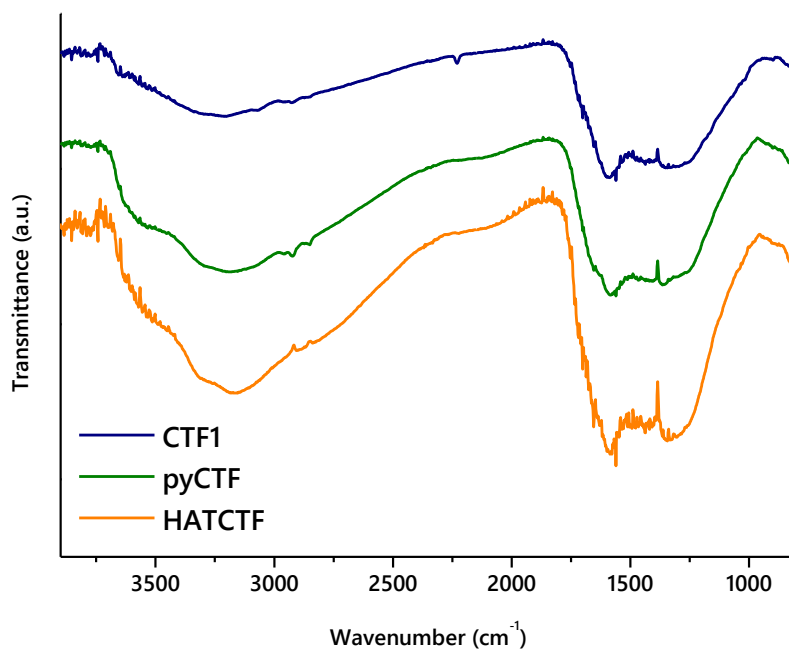# Diffuse Reflectance Infrared Fourier Transformed Spectroscopy (DRIFTS)

Figure S5: FTIR-DRIFTS spectra of CTF1, pyCTF and HATCTF. The broad peaks at around 1570 cm^{-1} and 1350 cm^{-1} were ascribed to triazine ring vibrations. The absence of a nitrile peak around 2230 cm^{-1} indicates the successful trimerization of the nitrile-containing monomer.
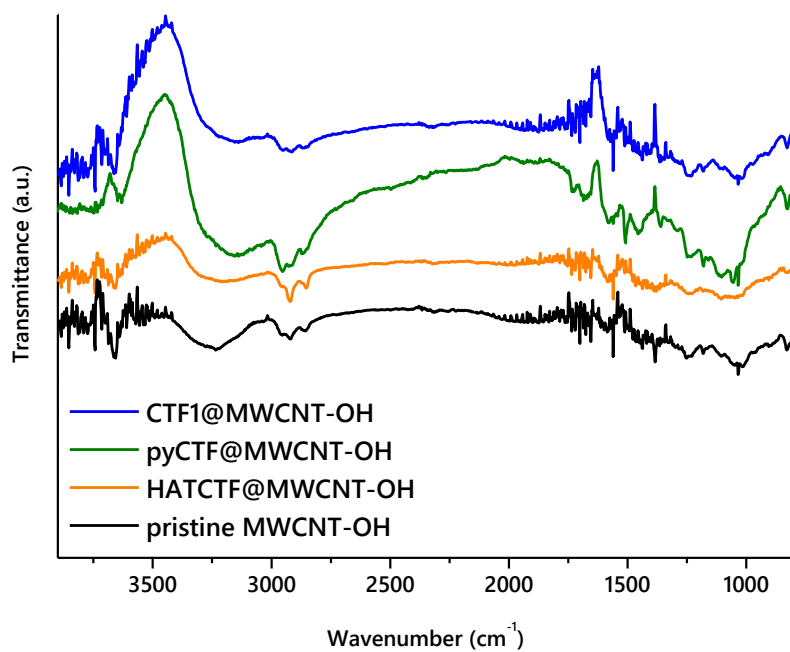
Figure S6: FTIR-DRIFTS spectra of CTF1@MWCNT-OH, pyCTF@MWCNT-OH and HATCTF@MWCNT-OH
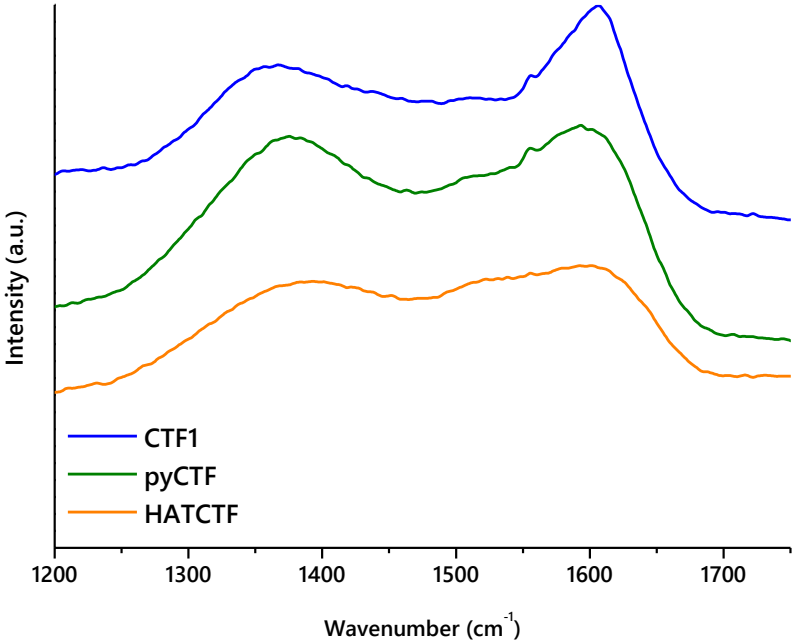
Raman Spectroscopy

Figure S7: Detail of Raman spectra of CTF1, pyCTF and HATCTF. A broad D-band at around 1350 cm^{-1} and G-band at around 1600 cm^{-1} can be discerned.
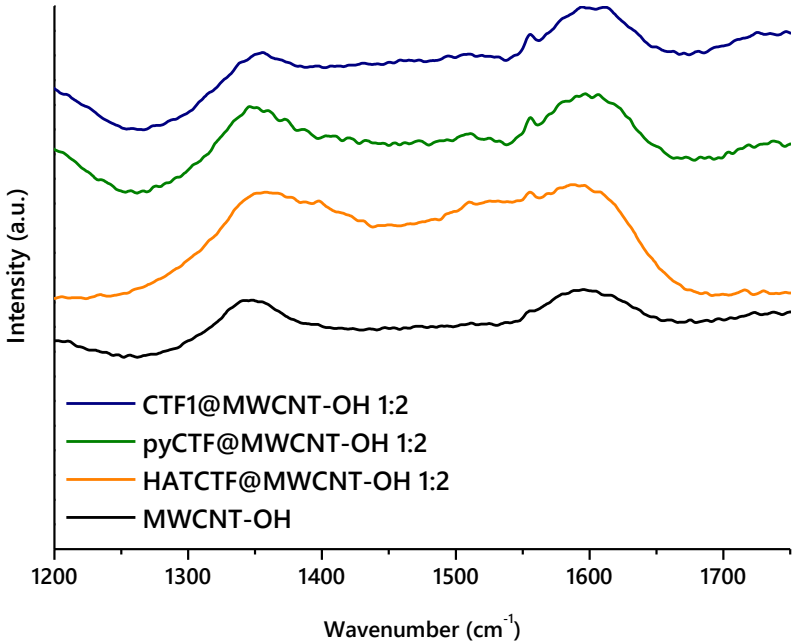

Figure S8: Detail of Raman spectra of CTF1@MWCNT-OH, pyCTF@MWCNT-OH and HATCTF@MWCNT-OH. A broad D-band at around 1350 cm^{-1} and G band at around 1600 cm^{-1} can be discerned.

X-ray Photoelectron Spectroscopy (XPS)

	C (at%)	O (at%)	N (at%)	Na (at%)	F (at%)	Si (at%)	Cl (at%)	Zn (at%)
MWCNT-OH	95.58	3.96		0.45				
CTF1@MWCNT-OH	92.19	3.32	3.6		0.73	0.15		
pyCTF@MWCNT-OH	91.78	2.81	4.48		0.46		0.31	0.15
HATCTF@MWCNT-OH	88.53	3.7	6.32		1.3			0.15

Table S1: XPS elemental atomic percentages of MWCNT-OH and hybrid materials
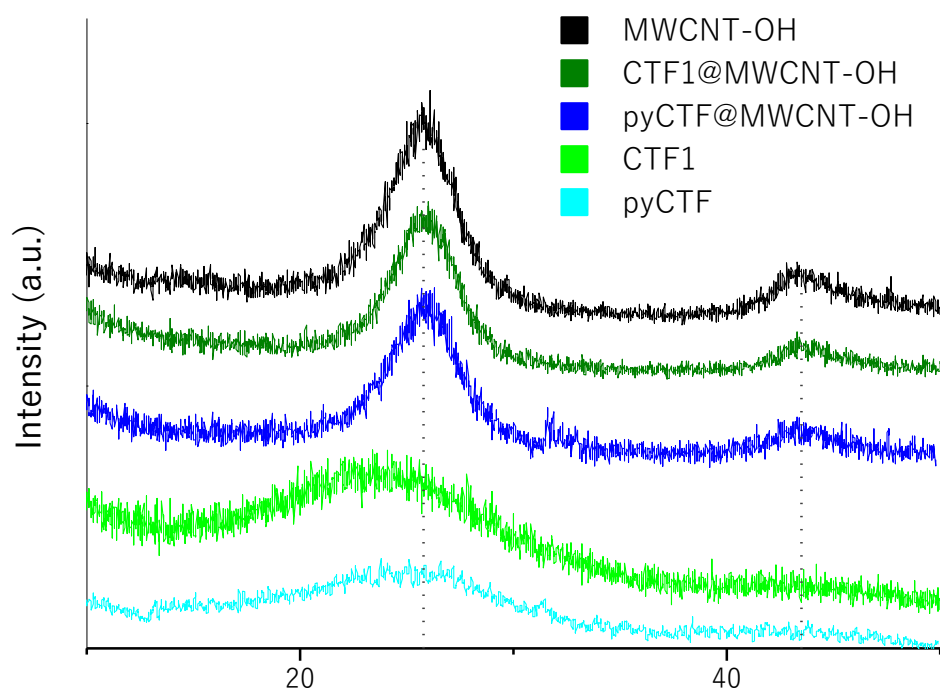
X-Ray Diffraction (XRD)

Figure S9: XRD patterns of MWCNT-OH, CTF1, pyCTF, CTF1@MWCNT-OH and pyCTF@MWCNT-OH

Scanning Transmission Electron Microscopy combined with Energy Dispersive X-ray spectroscopy (STEM-EDX)
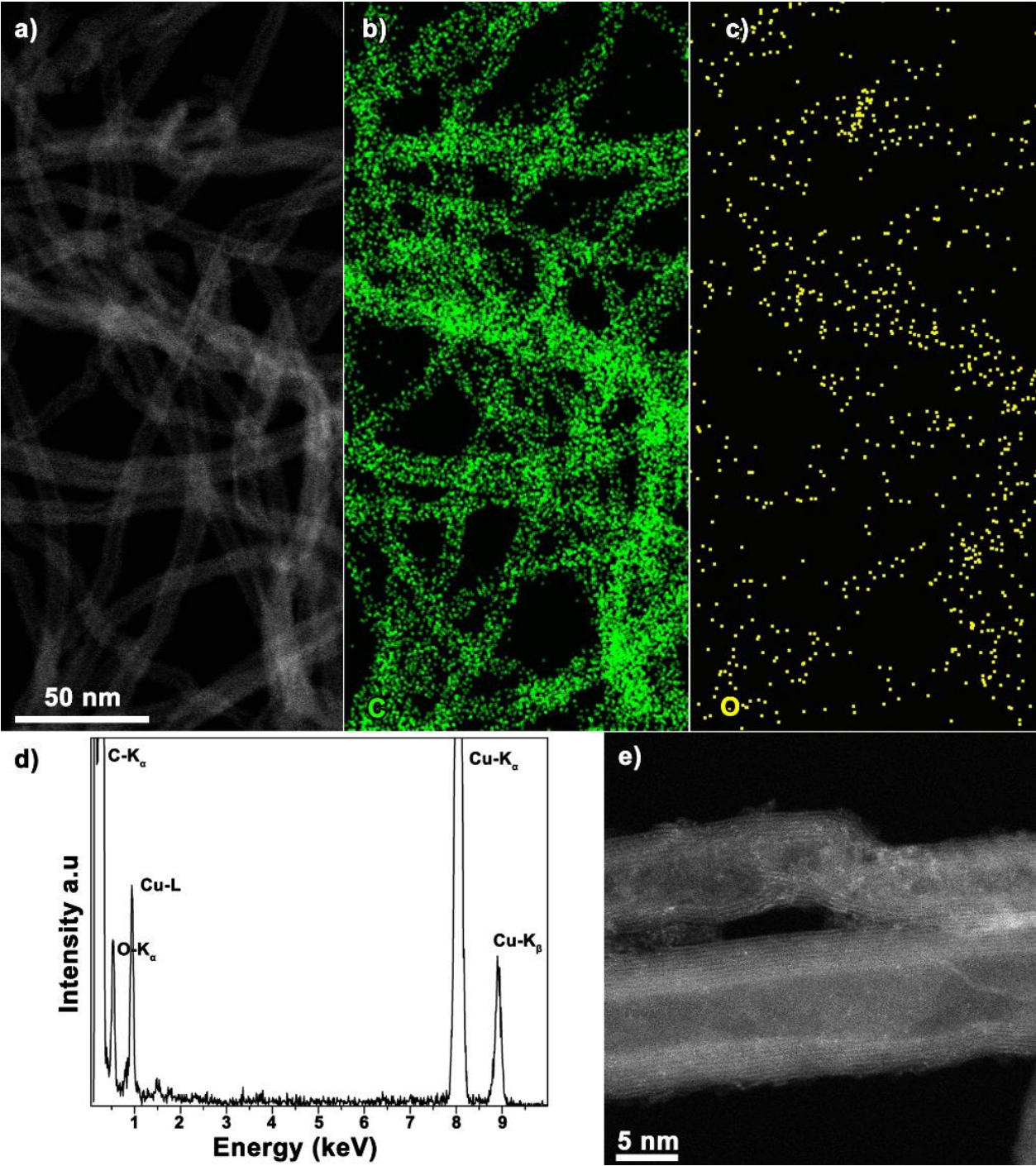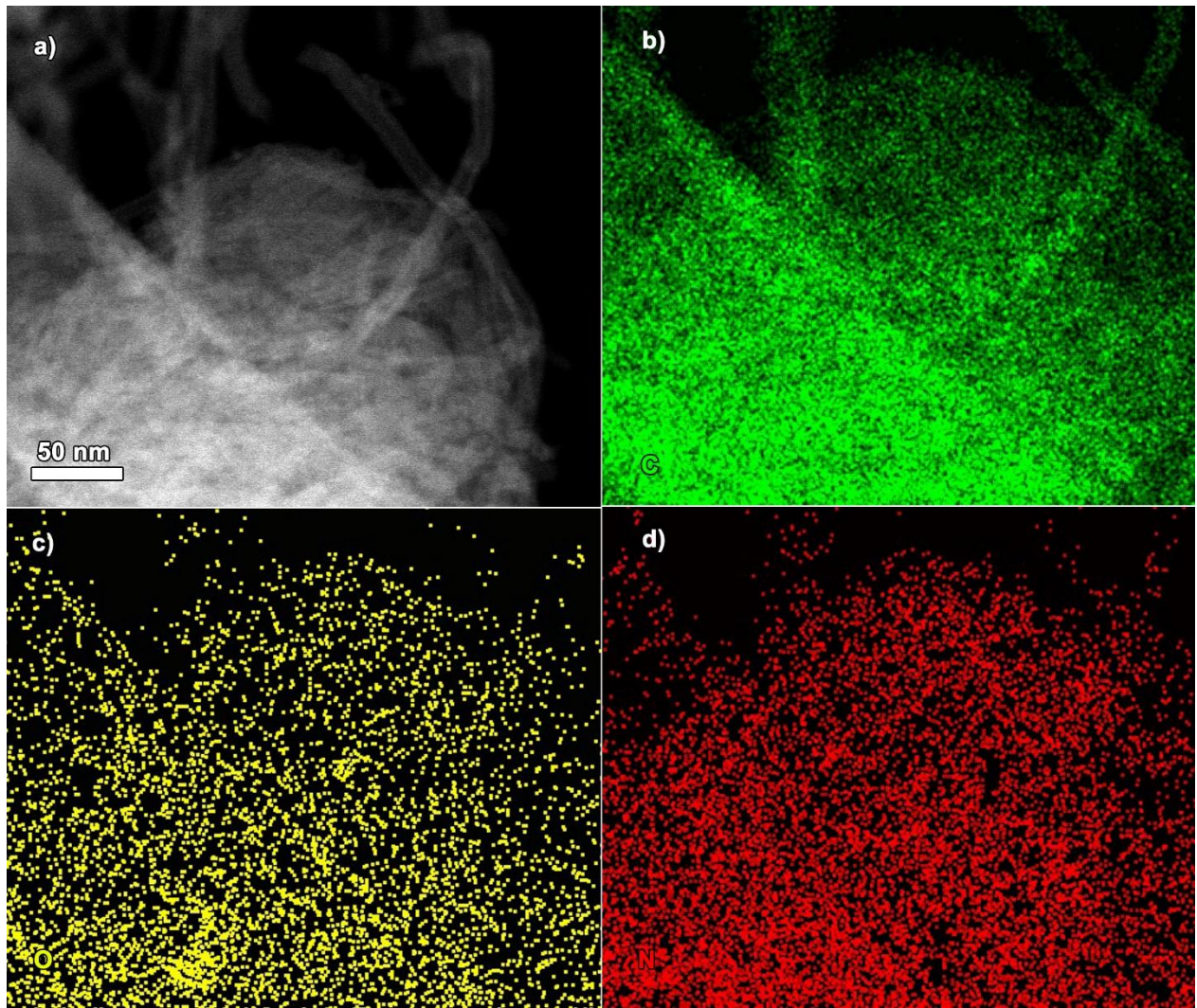

Figure S10: STEM-EDX of MWCNT-OH

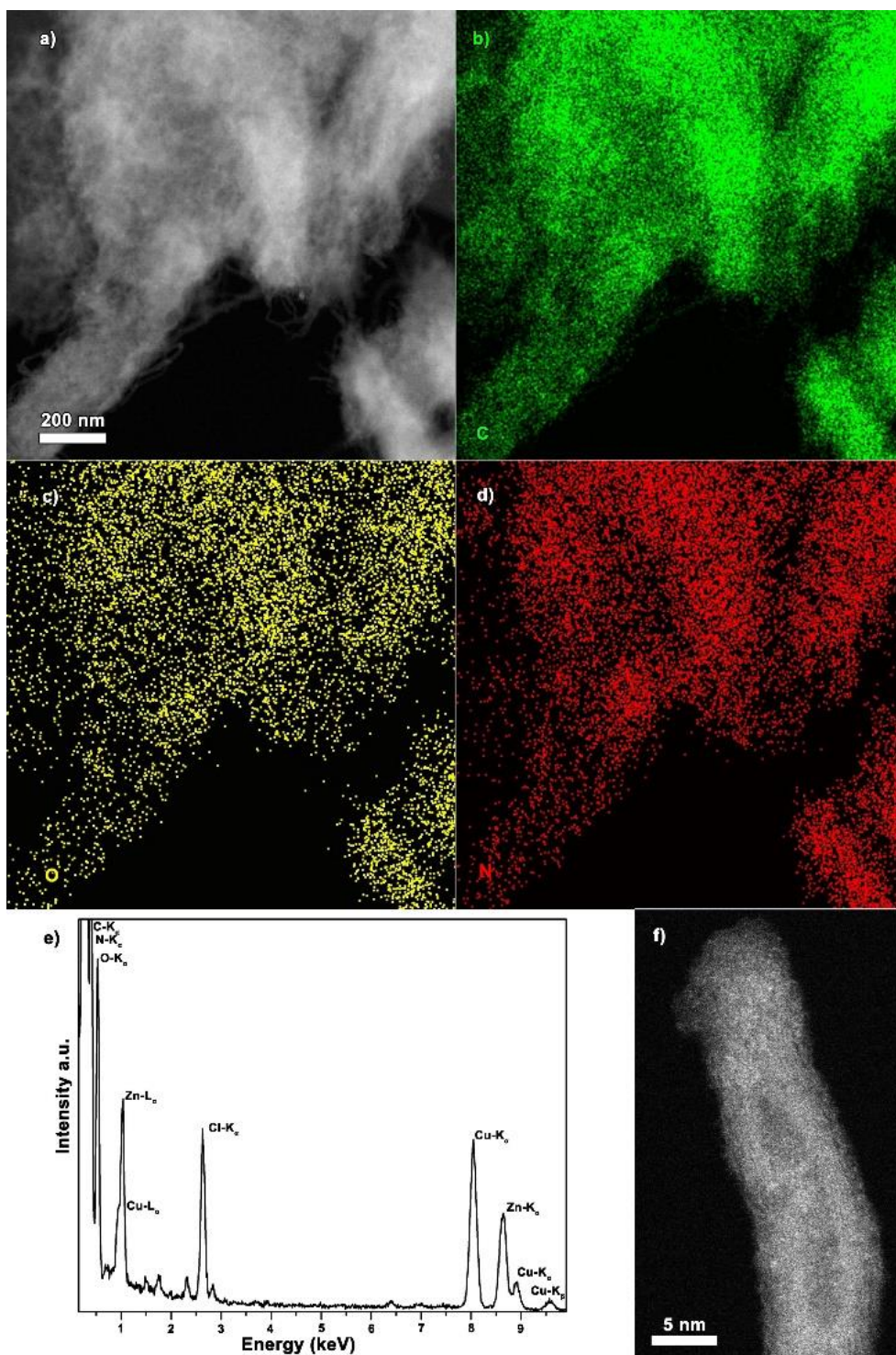Figure S11: STEM-EDX of HATCTFMWCNT-OH

Figure S12: STEM-EDX of pyCTF@MWCNT-OH

II. Electrochemical measurements

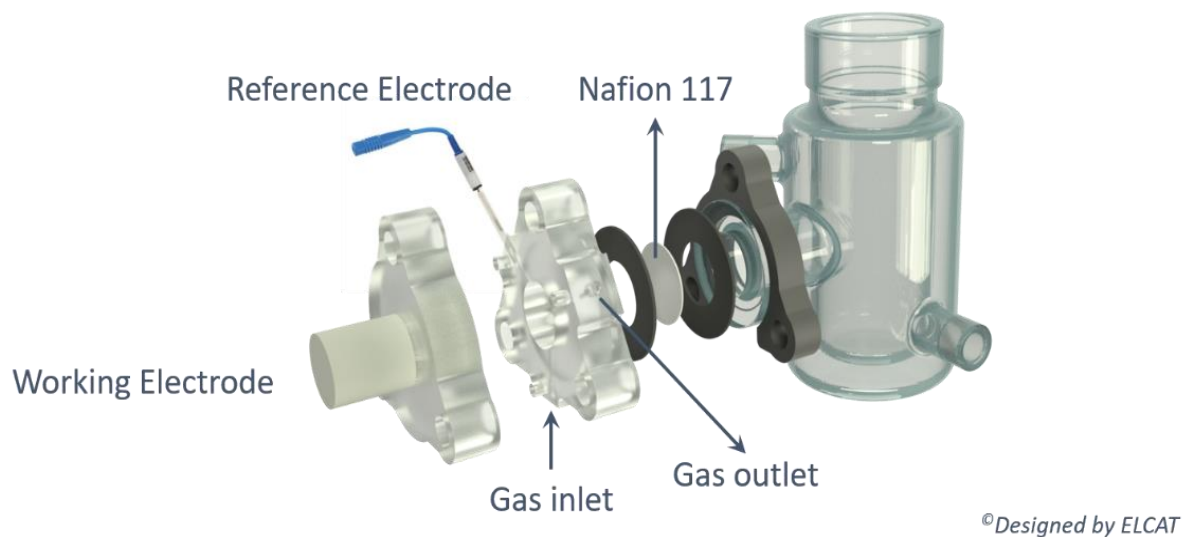## Electrochemical setup

Figure S13: The electrochemical H-type setup used for the electrochemical measurements.

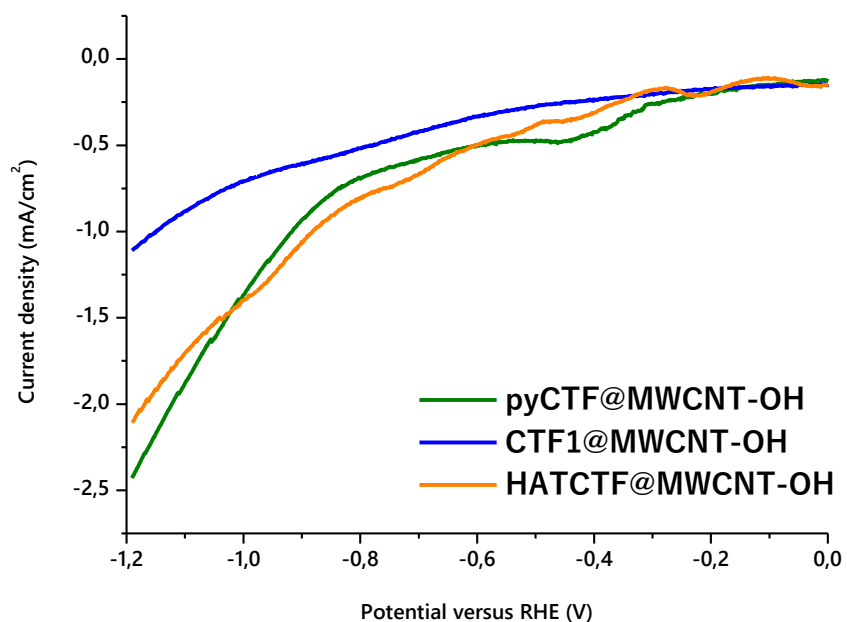## Linear Sweep Voltammetry (LSV)

Figure S14: LSV curves of pyCTF@MWCNT-OH, CTF1@MWCNT-OH and HATCTF@MWCNT-OH. Recorded in 0.1 M KHCO3 at 5 mV/s
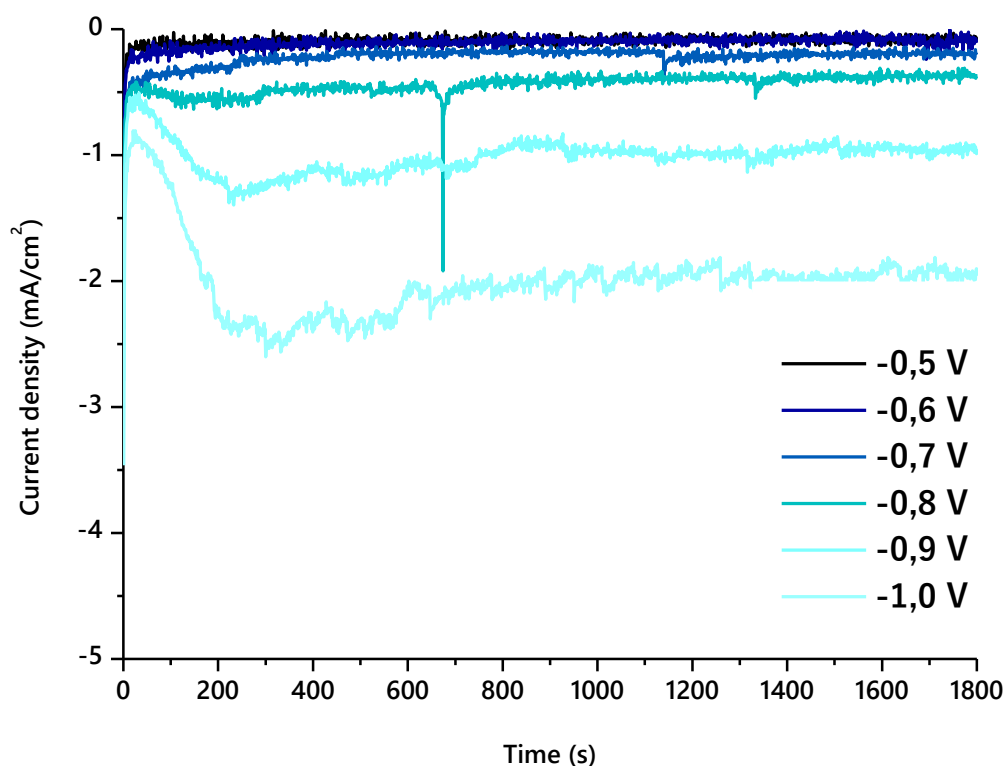
Chronoamperometry (CA)

Figure S15: Chronoamperometries of pristine carbon nanotubes. Recorded in 0.1 M KHCO$_3$.
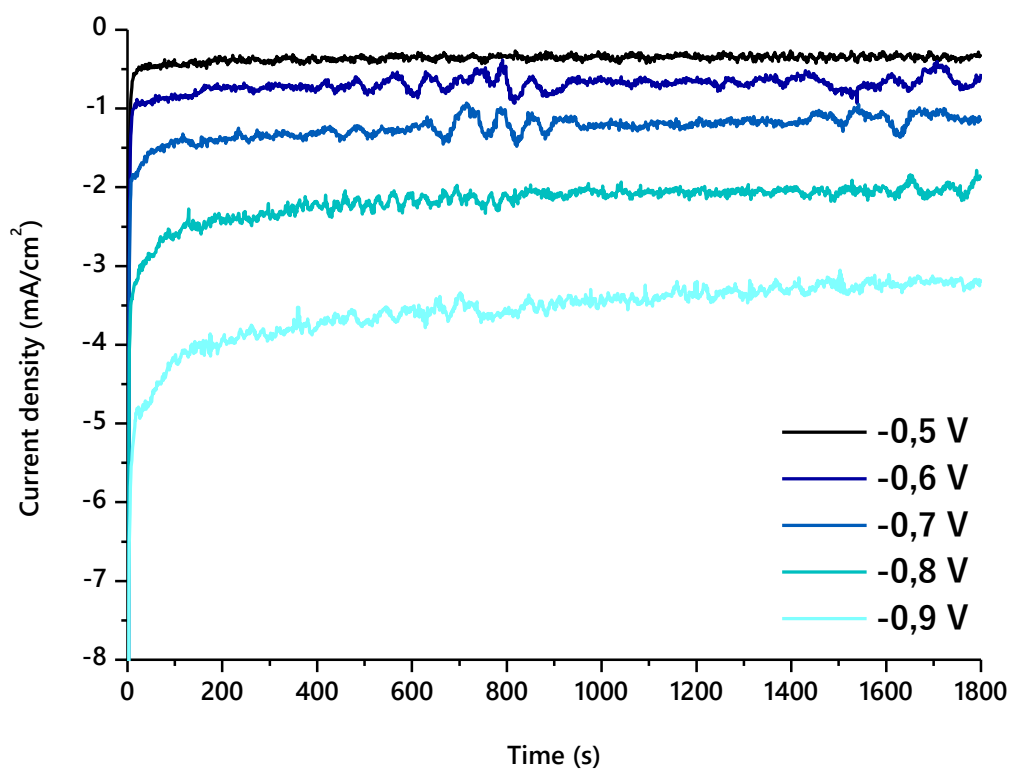All potentials are expressed versus RHE.

Figure S16: Chronoamperometry curves of HATCTF@MWCNT-OH. Recorded in 0.1 M KHCO$_3$.
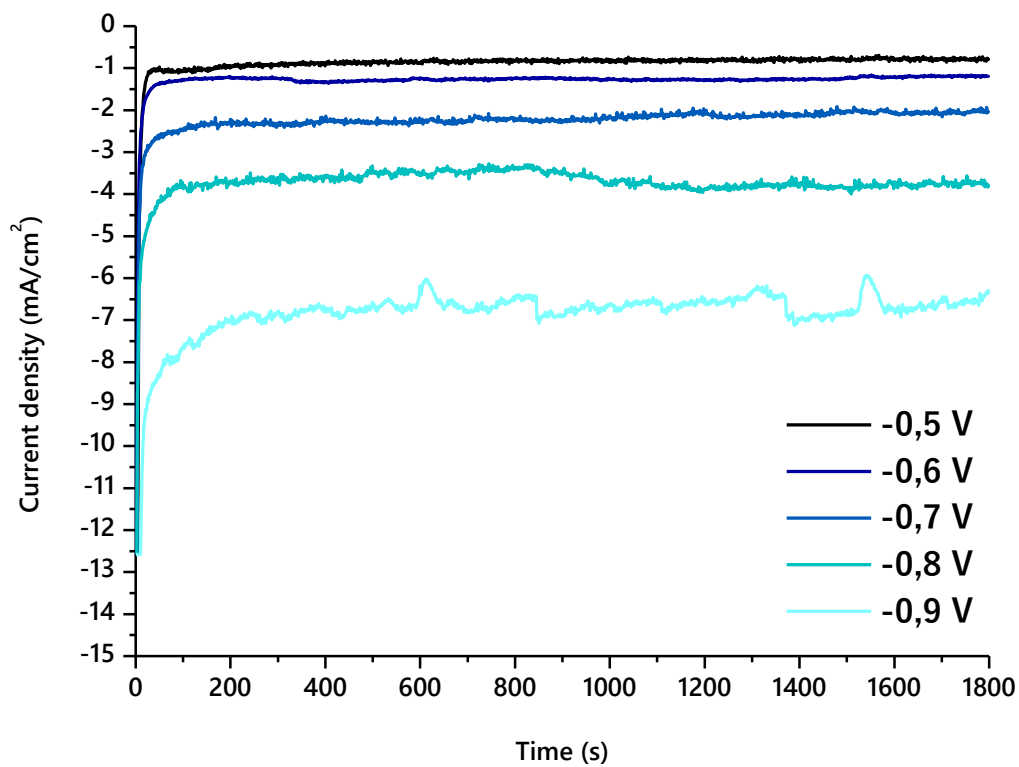All potentials are expressed versus RHE.

Figure S17: Chronoamperometry curves of pyCTF@MWCNT-OH. Recorded in 0.1 M KHCO$_3$. All potentials are expressed versus RHE.
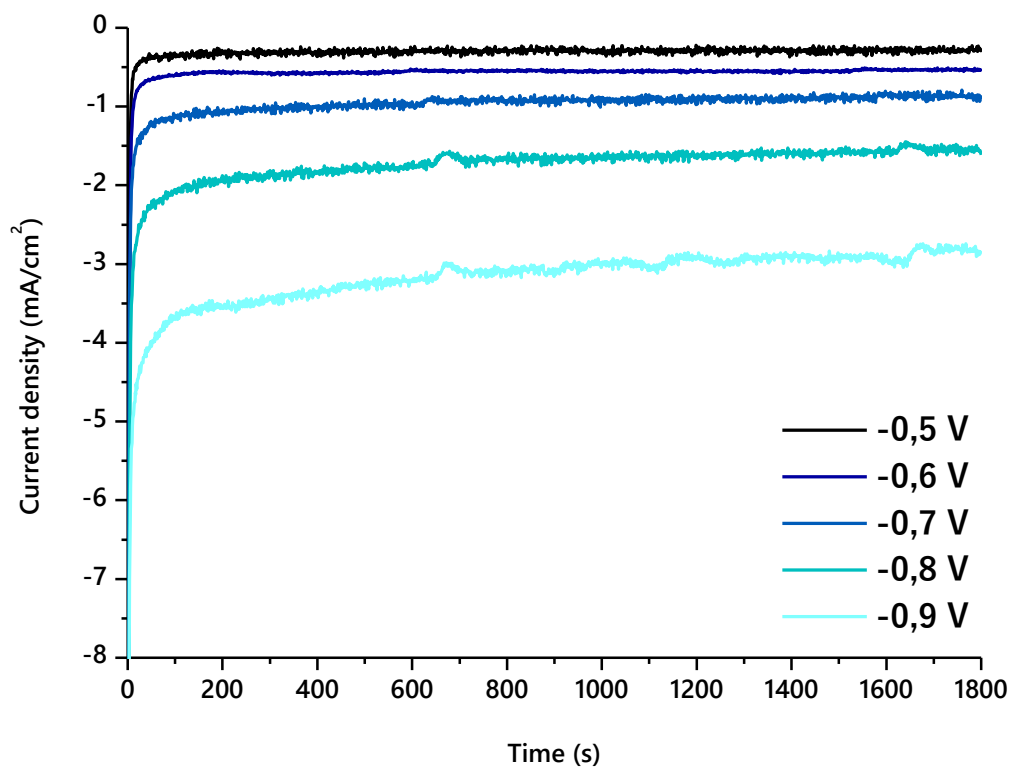

Figure S18: Chronoamperometry curves of CTF1@MWCNT-OH. Recorded in 0.1 M KHCO$_3$. All potentials are expressed versus RHE.
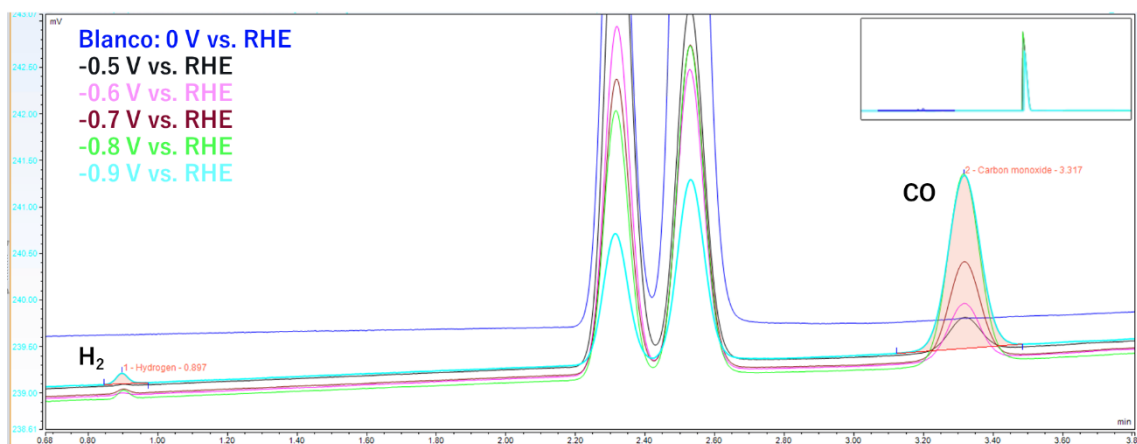
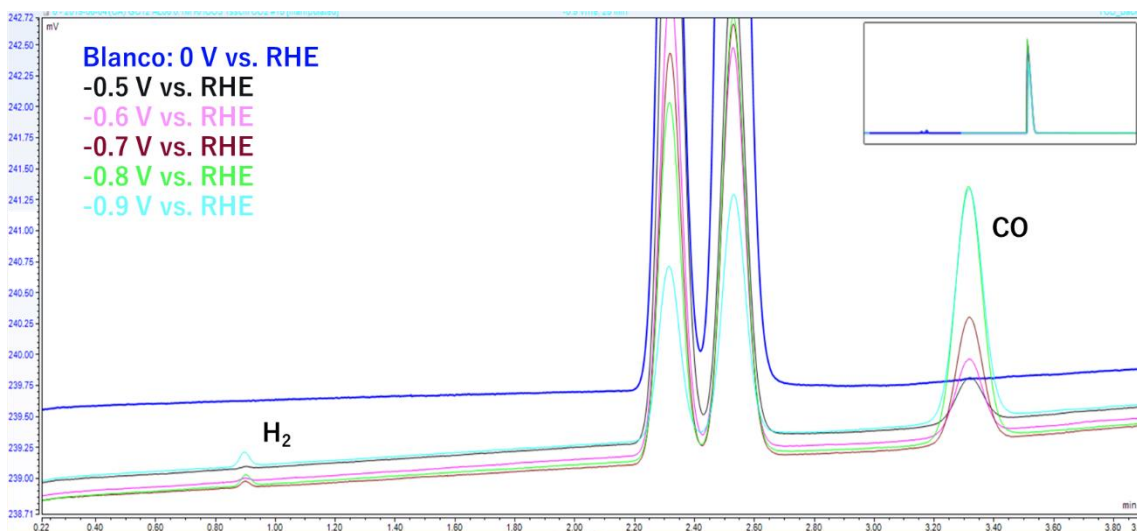Figure S19: Detail of the chromatogram of CTF1@MWCNT-OH

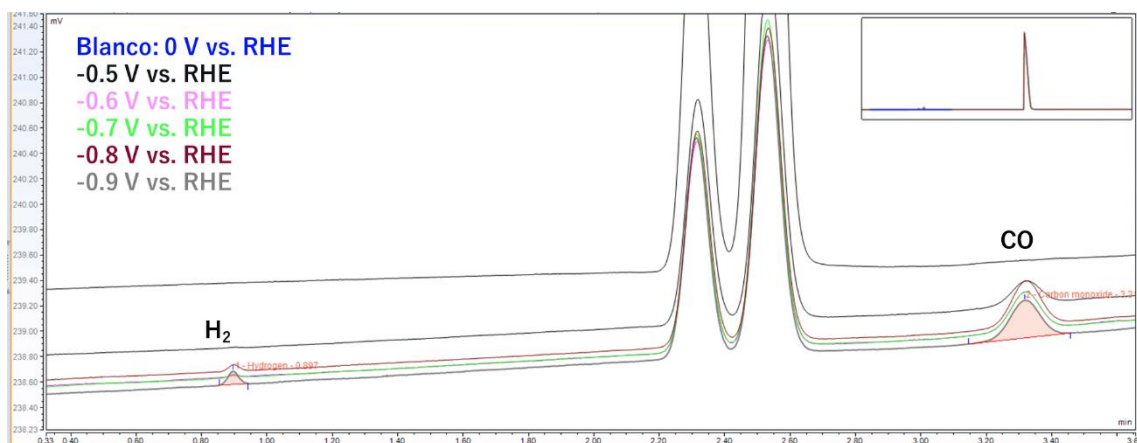Figure S20: Detail of the chromatogram of pyCTF@MWCNT-OH

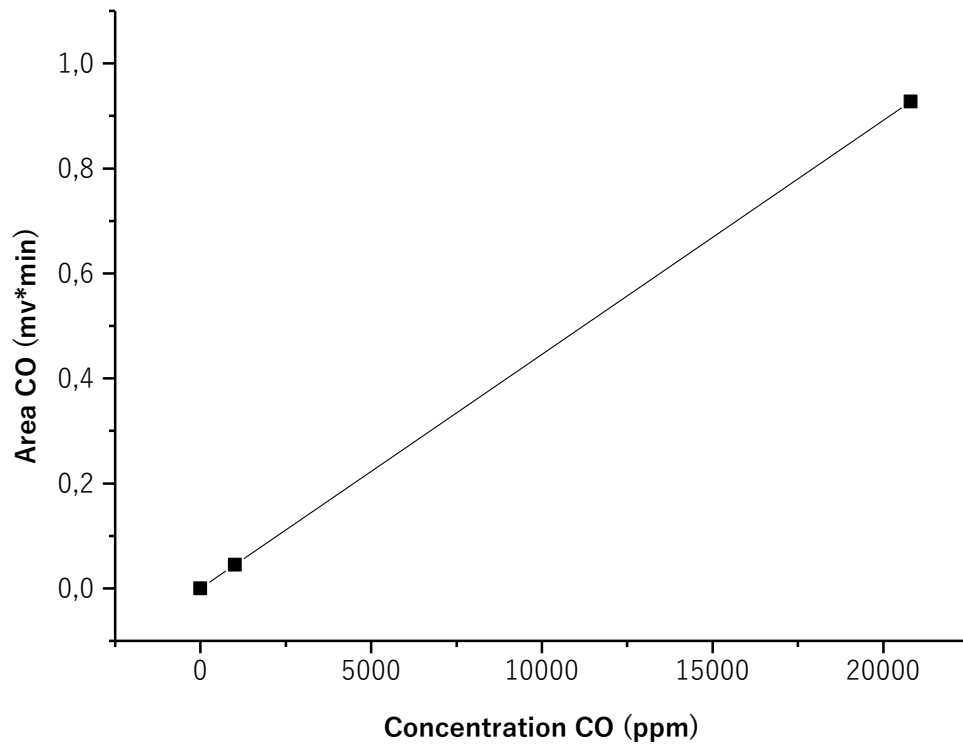Figure S21: Detail of the chromatogram of HATCTF@MWCNT-OH
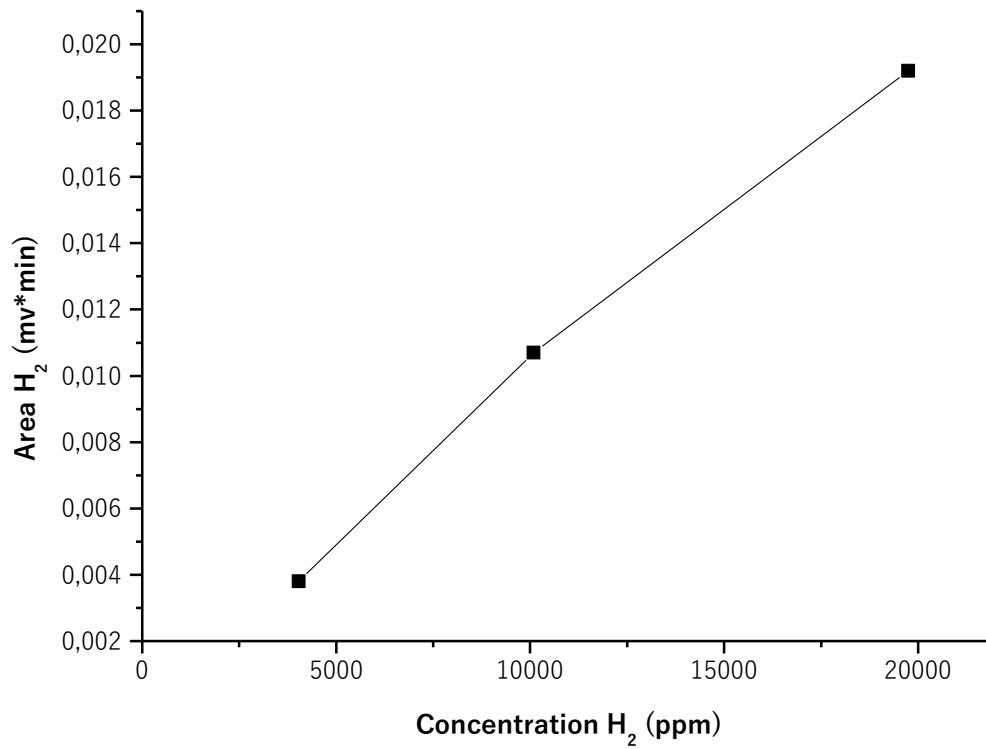
Figure S22: Calibration curve of CO

Figure S23: Calibration curve of H_2
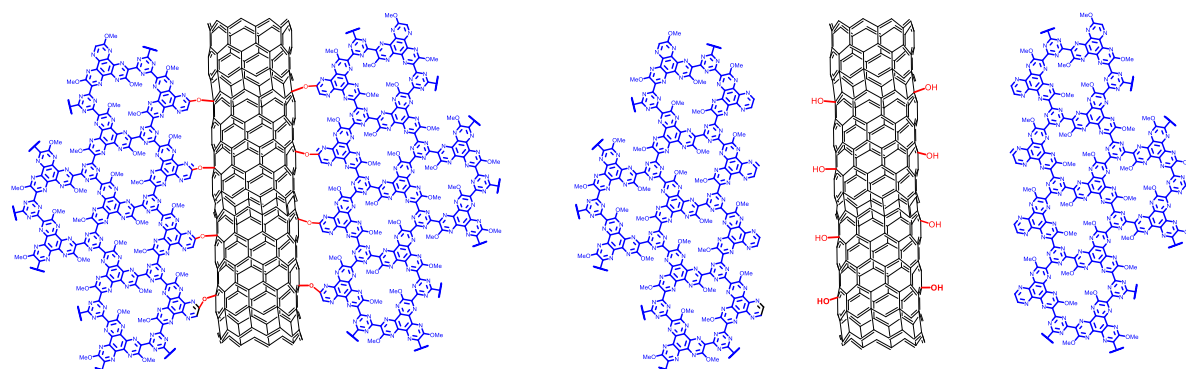
Calculation of Faradaic efficiencies

The Faradaic efficiencies were calculated based on the online GC measurements of the gaseous endproducts H_2 and CO during chronoamperometry according to the following equation:

$$FE = \frac{znF}{Q}$$

In which z is the number of electrons exchanged to form one molecule of the desired product (in the case of CO and hydrogen gas, z = 2), n is the molar amount of endproduct formed measured via GC, F is the Faraday constant and Q is the total charge generated during the process in the time up until the sample injection. Since no gaseous products other than CO and H_2 were detected by means of GC and no liquid products were detected with NMR and HPLC the total Faradaic efficiency was normalized to 100%.

III. Control experiments

Difference between HATCTF@MWCNT-OH and HATCTF + MWCNT-OH

HATCTF@MWCNT-OH   HATCTF + MWCNT-OH

Figure S24: Schematic interpretation of the structures of HATCTF@MWCNT-OH and HATCTF+MWCNT-OH

Inductively Coupled Plasma Mass Spectrometry (ICP-MS)

	Fe (g/kg)	Zn (g/kg)	Cu (mg/kg)	Mn (mg/kg)
HATCTF@MWCNT-OH	6.91	11.8	119	101
pristine MWCNT-OH	3.22	0.0604	76.9	88.8

Table S2: ICP-MS analysis of HATCTF@MWCNT-OH and pristine MWCNT-OH